Title: Experimental and theoretical investigation of the enantioselective hydrogenation of ethyl pyruvate with a Pt catalyst with new non-cinchona chiral modifiers

Author: José F. Ruggera Andrea B. Merlo Reinaldo Pis Diez Mónica L. Casella

PII: S1381-1169(16)30259-X
DOI: http://dx.doi.org/doi:10.1016/j.molcata.2016.07.009
Reference: MOLCAA 9943

To appear in: *Journal of Molecular Catalysis A: Chemical*

Received date: 17-3-2016
Revised date: 8-6-2016
Accepted date: 4-7-2016

Please cite this article as: José F.Ruggera, Andrea B.Merlo, Reinaldo Pis Diez, Mónica L.Casella, Experimental and theoretical investigation of the enantioselective hydrogenation of ethyl pyruvate with a Pt catalyst with new non-cinchona chiral modifiers, Journal of Molecular Catalysis A: Chemical http://dx.doi.org/10.1016/j.molcata.2016.07.009

Experimental and theoretical investigation of the enantioselective hydrogenation of ethyl pyruvate with a Pt catalyst with new non-cinchona chiral modifiers

José F. Ruggera*[,a], Andrea B. Merlo[a], Reinaldo Pis Diez[b], Mónica L. Casella[a]

a Centro de Investigación y Desarrollo en Ciencias Aplicadas "Dr. Jorge J. Ronco", CINDECA (Facultad de Ciencias Exactas, UNLP – CCT La Plata, CONICET), calle 47 N° 257 1900 La Plata, Argentina

b Centro de Química Inorgánica, CEQUINOR (Facultad de Ciencias Exactas, UNLP-CCT La Plata, CONICET) Bv. 120 e/60 y 64 N°1465, C. C. 962 - 1900 La Plata, Argentina

** corresponding author, e-mail: jfruggera@quimica.unlp.edu.ar*

Graphical abstract

NEW CHIRAL MODIFIERS FOR THE ORITO REACTION

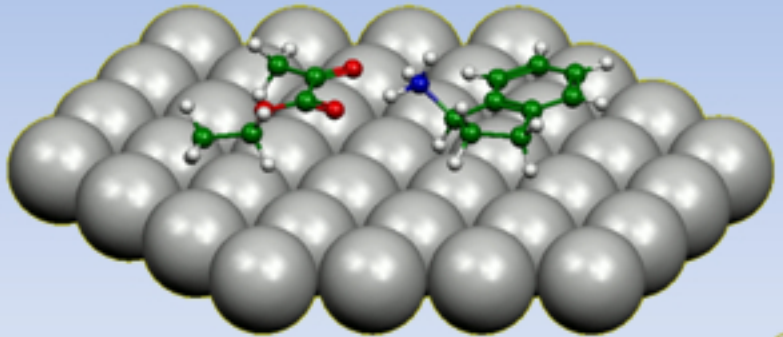

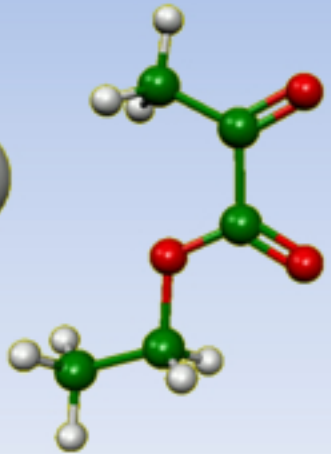

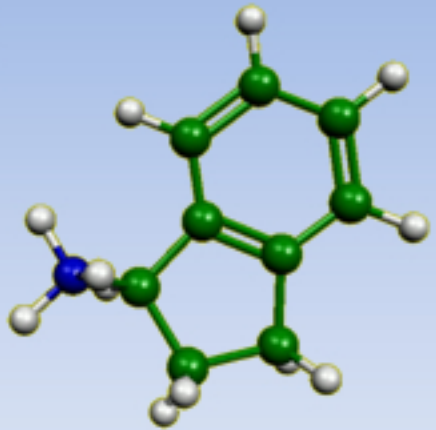

Highlights

Ethyl pyruvate was hydrogenated on a Pt/SiO_2 catalyst modified with chiral modifiers

An enantiomeric excess (*ee%*) of 63% was obtained with (S)-(+)-1-aminoindan.

Density Functional Theory calculations allowed predicting *ee%* obtained experimentally.

Low *ee%* for aminoindanol was explained by the noncovalent interaction approach.

ABSTRACT

The enantioselective hydrogenation of ethyl pyruvate using a Pt/SiO_2 catalyst modified with six different chiral modifiers was studied. The chiral modifiers chosen were: (S)-(+)-1-aminoindan, (R)-(-)-1-aminoindan, (1R,2S)-(+)-*cis*-1- amino-2-indanol, (1S,2R)-(-)-*cis*-1-amino-2-indanol, (S)-(+)-1-indanol and (R)-(-)-1-indanol.An excess of the (R) enantiomer of the product of 63% and 45% with (S)-(+)-1-aminoindan and (R)-(-)-1-aminoindan modifiers, respectively was obtained. When using (1S,2R)-(-)-*cis*-1-amino-2-indanol and (1R,2S)-(+)-*cis*-1-amino-2-indanol, the enantiomeric excess (*ee%*) obtained was 30% and 5%, respectively, while with both indanols *ee%* did not exceed 8%. Molecular modeling of the complex formed between the chiral modifier and ethyl pyruvate performed by DFT calculations allowed predicting the values of *ee%* obtained experimentally. The low *ee%* value obtained both aminoindanol chiral modifiers were used, could be explained by the analysis of non-covalent interactions (NCI) method. These calculations demonstrated the presence of an intramolecular hydrogen bond in the structure of these modifiers.

Keywords: enantioselectivity; ethyl pyruvate; non-cinchona modifiers; DFT; platinum

INTRODUCTION

The growing demand for enantiomerically pure compounds in the field of pharmaceutical and agrochemical industries has increased the importance of optically active compounds synthesis [1-3].

In this sense, asymmetric catalysis has become a challenging subject in the field of catalysis over the last years. One of the very interesting heterogeneous catalytic processes, named *"classical approach"*, is enantioselective hydrogenation using metallic catalysts modified with chiral compounds [4, 5]. This methodology allowed the development of the most widely employed heterogeneous chiral catalysts: Ni catalyst modified with sodium tartrate/NaBr [6, 7] and Pt(Pd) catalyst modified with alkaloids of the cinchona group used to hydrogenate α-ketoesters ([8] and references therein). The enantioselective hydrogenation of α-ketoesters constitutes a useful reaction at industrial level since the reaction products, α–hydroxyesters, are key intermediates in the synthesis of biologically active compounds [9]. Japanese researchers were the first ones to perform studies in the field of asymmetric catalysis using Pt/C catalysts modified with cinchonidine for the hydrogenation of ethyl pyruvate, obtaining high optical yields [10]. In the last three decades, these reactions have been studied for the enantioselective hydrogenation of a large number of α-ketoesters and α-diketones [11-16].

With respect to the nature of the chiral modifier, when analyzing the performance of Pt-based catalysts modified with cinchonidine, the effectiveness in obtaining a high enantiomeric excess is assigned to the structure of this modifier. Three factors are crucial: a group capable of anchoring the molecule onto the surface of the metallic catalyst, the presence of a basic nitrogen atom near the stereogenic center, and a chiral center [10].

There is clear evidence that cinchonidine adsorbs on the metal surface via the aromatic quinoline π–system [17-20] forming the chiral site. Methyl pyruvate, one of the most widely molecules used as substrate in hydrogenation reactions, adsorbs on these modified chiral sites either by the oxygen lone pairs [21,22] or the π-bonding of the C=O groups [23]. Hydrogen bond and donor–acceptor interactions between the modifier and selected functional groups of the substrate molecule control the adsorption mode of methyl pyruvate and facilitate the addition of hydrogen, thereby increasing the reactivity [24,25].The formation of a complex between the modifier and the substrate in a 1:1 stoichiometry is a key feature in this mechanism [26]. In this sense, many studies have been carried out aiming at understanding the role of the chiral modifier structure in the mechanism of Orito's reaction. Tálas and Margitfalvi have written a very complete review article, in which they describe the behavior of natural alkaloids, their synthetic derivatives and analogues as chiral templates in the heterogeneous catalytic asymmetric hydrogenation of activated ketones [27]. The authors demonstrated that different types of activated ketones could be successfully hydrogenated by use of different chiral templates, being cinchonidine the most usable chiral modifier for the asymmetric hydrogenation of a wide variety of activated ketones. Kukula et al. also studied the structural effects in the chiral base employed in the Pd-induced enantioselective deprotection–decarboxylation of β-ketoesters. Various chiral amines and amino alcohols were tested in the reaction, achieving enantioselectivities up to 60% quinine and quinidine [28].

In this work, the enantioselective hydrogenation of ethyl pyruvate using a Pt/SiO_2 catalyst modified with (S)-(+)-1-aminoindan, (R)-(-)-1-aminoindan, (1R,2S)-(+)-*cis*-1-amino-2-indanol and (1S,2R)-(-)-*cis*-1-amino-2-indanol was studied. The chosen modifiers are simpler and more rigid than cinchonidine, but still present its main

structural features. (S)-(+)-1-indanol and (R)-(-)-1-indanol were also selected as chiral modifiers. All the modifiers employed are represented in Scheme 1. The interaction between the modifiers and the ethyl pyruvate molecule was also modeled using tools from the density functional theory (DFT).

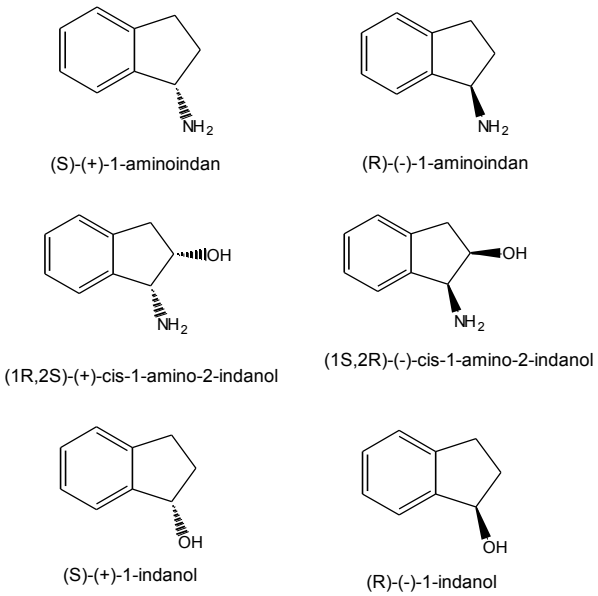

Scheme 1. Chemical structures of the chiral modifiers studied

EXPERIMENTAL AND COMPUTATIONAL METHODS

Catalyst preparation and modification

The monometallic catalyst, Pt/SiO_2, was prepared by ion exchange, using SiO_2 as support (Aerosil Degussa 180 m^2 g^{-1}), previously treated with $NH_4OH_{(aq)}$. The solid obtained was reduced and modified with (S)-(+)-1-aminoindan, (R)-(-)-1-aminoindan, (1R,2S)-(+)-*cis*-1-amino-2-indanol, (1S,2R)-(-)-*cis*-1-amino-2-indanol, (S)-(+)-1-indanol and (R)-(-)-1-indanol (Aldrich), according to the previously published procedure [29].

Catalyst characterization

The platinum content was determined with the aid of an atomic emission spectrometer Perkin Elmer AAnalyst 100 after dissolving the solid. The distribution of metallic particle size was determined by transmission electron microscopy (TEM) using a JEOL 100 CX instrument. To estimate the mean particle size, the particles were considered spherical, and the second moment of the distribution was employed. The expression used for the calculation was:

$$d = \frac{\sum n_i d_i^3}{\sum n_i d_i^2}$$

where n_i is the number of particles with d_i size. Temperature-programmed reduction (TPR) tests were carried out in a conventional reactor with a feeding flow of 20 cm^3 min^{-1} (10% H_2 in N_2) at a heating rate of 10 K min^{-1}, from room temperature to 1073 K. H_2 consumption during reduction was analyzed on line with a Shimadzu GC-8A gas chromatograph with a thermal conductivity detector (TCD).

Hydrogenation reactions

The hydrogenation reaction of 1 mL ethyl pyruvate (Aldrich) (**Figure 1**) was performed in an autoclave type reactor (Autoclave Engineers), at 1.0 MPa H_2 pressure and at a temperature of 273 K, using 0.25 g catalyst and 60 mL of 2-propanol as solvent.

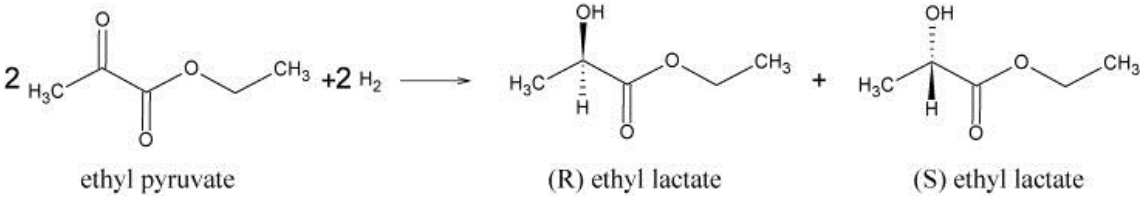

ethyl pyruvate (R) ethyl lactate (S) ethyl lactate

Figure 1. Enantioselective hydrogenation of ethyl pyruvate to (R) and (S)-ethyl lactate

The reaction advance was followed by gas chromatography in a Varian GC 3800 chromatograph equipped with a capillary column (CP–Chirasil–Dex CB) and a FID

detector. The only reaction products obtained, (R) and (S)-ethyl lactate, were completely separated under the analysis conditions used. The enantiomeric excess (*ee%*) was calculated using the following expression:

$$ee\% = \frac{([R]-[S])}{([R]+[S])} \times 100 \quad (1)$$

where [R] and [S] are the concentrations of the *R* and *S* enantiomers, respectively.

Theoretical calculations

The proton affinity (PA) of the chiral modifiers was calculated as:

$$Modifier + H^+ \rightarrow (Modifier - H^+) \quad (2)$$

and it was characterized by the enthalpy change at standard conditions (273 K, 1 bar). For (S)-(+)-1-aminoindan, (R)-(-)-1-aminoindan, (1R,2S)-(+)-*cis*-1-amino-2-indanol and (1S,2R)-(-)-*cis*-1-amino-2-indanol molecules, the amino group was evaluated as the protonation site, while for (S)-(+)-1-indanol and (R)-(-)-1-indanol molecules, the alcohol group was chosen. The equilibrium structures for the neutral and protonated molecules of the different modifiers were obtained with the BLYP exchange-correlation functional [30, 31] and a basis set of triple-ζ quality, augmented with polarization functions. The eigenvalues of the Hessian matrix of the total electronic energy with respect to the nuclear coordinates were also calculated to confirm whether the optimized geometries correspond to minima or saddle points on the potential energy surface of the molecules. All calculations were performed with the Amsterdam Density Functional (ADF) software [32].

Due to the complexity of the metallic catalyst/chiral modifier/substrate/solvent system, a number of simplifications were made in order to carry out the calculations. Thus, the contribution of the metal was not explicitly considered in this model since it involves a large computational demand. In addition, it was considered that the molecules of all the

studied modifiers adsorb onto the metal surface through a link involving their benzene system, so that they remain substantially parallel to the surface.

Both the *cis* and *trans* conformations of the substrate (ethyl pyruvate) were considered, and their geometries were optimized. The geometries of the protonated forms of the modifiers were also optimized. Finally, different starting geometries for the substrate–modifier complex were modeled, four for every modifier, pro-R-*cis*, pro-R-*trans*, pro-S-*cis* and pro-S-*trans*. The geometries of the substrate–modifier complexes were optimized at the BLYP/TZP level theory.

The solvent effect was taken into account through the implementation of the COSMO model [33].

The difference in the Gibbs free energy of formation (ΔG_f) of all the complexes was calculated as the difference between the Gibbs free energy of the modifier–substrate complex and their isolated components:

$$\Delta G_f = G_{complex} - \left(G_{modifier} + G_{substrate}\right) \quad (3)$$

The theoretical enantiomeric excess was calculated taking into account the relative abundance of each complex at 273 K, 1 bar of pressure and in a 2-propanol medium. This relative abundance was calculated from the Gibbs free energies of formation using a Maxwell-Boltzmann distribution:

$$\frac{N_i}{N} = \frac{e^{-\Delta G_{fi}/RT}}{\sum_i e^{-\Delta G_{fi}/RT}} \quad (4)$$

The noncovalent interaction (NCI) approach was used to visualize possible intramolecular hydrogen bonding [34]. The NCI approach is based on the study of electron densities and their gradient in low electron density regions and small reduced gradients. The zones where the reduced gradient s(ρ) is close to zero are typical of

noncovalent interactions. In order to visualize it in the molecule, isosurfaces are plotted and colored considering the sign of the second eigenvalue of the Hessian matrix λ_2 (second derivative of the electron density as a function of nuclear coordinates). The blue isosurface zones correspond to positive λ_2 values, which represent the areas where repulsive interactions occur. The red zones, which correspond to negative λ_2 values, identify regions with attractive noncovalent interactions, such as hydrogen bonds. Green isosurface zones are those where the value of λ_2 is close to zero and indicate regions involving weak delocalized interactions [35,36]. GABEDIT software was used to draw all molecule graphs and do the NCI analysis [37]

RESULTS AND DISCUSSION

Catalyst characterization

The atomic absorption results show a Pt content of 2 wt%. The prepared catalyst was characterized by TEM in order to evaluate the metallic particle size distribution. The micrograph presented in **Figure 2** indicates that the metallic particles of the Pt/SiO_2 catalyst are well dispersed on the support and a mean particle size of about 6.5 nm was calculated using the expression given in the experimental section. The size of the metal particles is very important in the development of active catalysts for enantioselective hydrogenations, since there is plenty of evidence that they are very sensitive to this parameter. It has been reported in the literature that the hydrogenation of ethyl pyruvate using cinchodine as modifier requires a Pt particle size of at least 3 nm [38]. When a larger substrate such as 1-phenyl-1,2-propanodione is used, a Pt particle size of 4 nm when the support is Al_2O_3 and 3.8 nm when the support is SiO_2 is required [39].

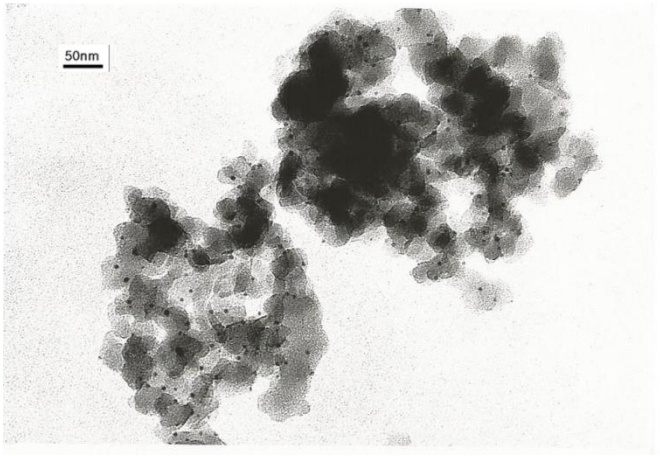

Figure 2. TEM image of Pt/SiO_2 catalyst.

With respect to the TPR test, the diagram (not shown) presented two major peaks of H_2 consumption: one reduction peak at a lower temperature, around 460 K, and the other at a higher temperature (*ca.* 715 K). According to the literature, the low temperature peak can be assigned to the presence of Pt (IV) species, generated during the calcination pretreatment. The high temperature peak may be assigned to species of the type Pt-(O-Si≡)$_y^{n-y}$ (n = 2+ or 4+), formed through the interaction of the metallic precursor and the support [40]. The peaks obtained were broad and presented shoulders, which could be due to the different environment of the ions on the support surface.

Hydrogenation of ethyl pyruvate

Figure 3 and **Table 1** present the results achieved in the racemic and enantioselective hydrogenation of ethyl pyruvate employing the Pt/SiO_2 catalyst, using 2-propanol as solvent, at 273 K. For the enantioselective hydrogenation experiments, the catalyst was modified with different chiral inducers. The adsorption of small amounts of a chiral modifier on the surface of the metallic catalyst generates a *"chiral catalytic site"* suitable for the interaction of the substrate to be hydrogenated. Besides, in most of the cases, the modifier leads to a significant increase in the reaction rate, compared to what

occurs with the unmodified catalyst. This rate acceleration has been traditionally observed for the hydrogenation of several prochiral carbonyl compounds in the presence of different modifiers of the cinchona alkaloids [41,42]. When analyzing the activity of the different catalytic systems employed in this work, it is possible to observe that the (S)-(+)-1-aminoindan and (R)-(-)-1-aminoindan present an almost complete conversion for a reaction time of about 30 min. These results are comparable with those previously obtained with the same Pt/SiO_2 catalyst modified with cinchonidine [43]. When the modifiers (1S,2R)-(-)-*cis*-1-amino-2-indanol and (1R,2S)-(+)-*cis*-1-amino-2-indanol are used, the conversion does not reach 60% or 30%, respectively, for the same reaction time **(Figure 4)**. On the other hand, with the (S)-(+)-1-indanol and (R)-(-)-1-indanol modifiers, 65% and 55% conversion values are obtained, respectively, for 30 min of reaction. The significant difference in the hydrogenation rate between aminoindan and aminoindanol modifiers can be interpreted on the basis of the existence of an important interaction between –OH and $–NH_2$ groups in the aminoindanol molecule [44,29].

Table 1: Racemic and enantioselective hydrogenation of ethyl pyruvate.

Modifier	***ee%*[a]**	**r_i[b]**
------	0	2.96
(S)-(+)-1-aminoindan	63 (R)	7.35
(R)-(-)-1-aminoindan	45 (R)	6.96
(1R,2S)-(+)-cis-1-amino-*2*-indanol	< 5 (R)	1.89
(1S,2R)-(-)-cis-1-amino-*2*-indanol	30 (R)	3.59
(S)-(+)-1-indanol	< 5 (S)	3.68
(R)-(-)-1-indanol	8 (S)	3.38

Reaction conditions: 250 mg of 2 wt% Pt/SiO_2 catalyst; 1.0 MPa of H_2 pressure; solvent: 2-propanol; 273 K.

[a]Enantiomeric excess calculated with equation (1) at 80% conversion. Absolute configuration in brackets.

[b]Reaction rate estimated between 0% and 10% conversion. Expressed as mmol g^{-1}_{Ptsup} sec^{-1}.

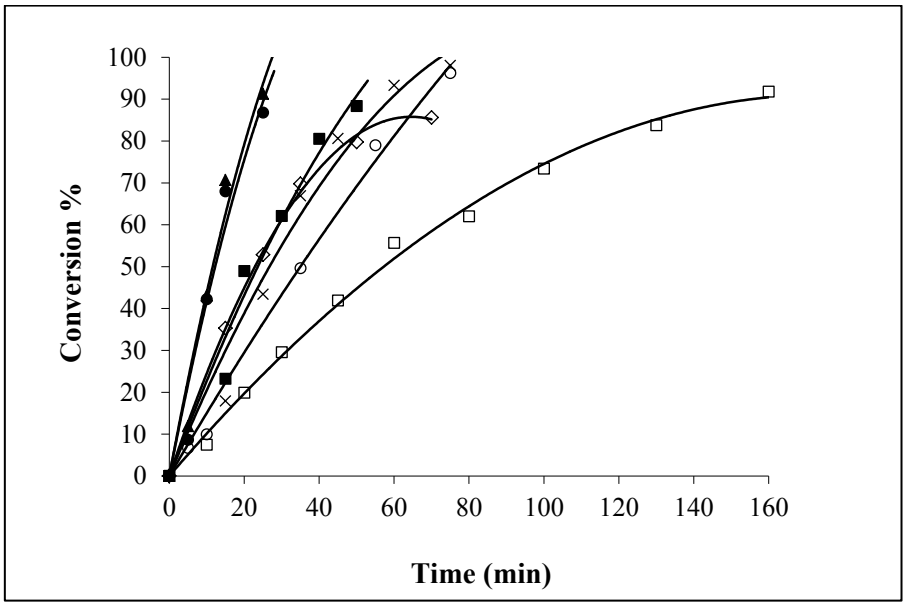

Figure 3. Hydrogenation reaction of ethyl pyruvate in 2-propanol. Conversion as a function of time for the Pt/SiO_2 catalyst without modifier (×) and modified with: (S)-(+)-1-aminoindan (▲), (R)-(-)-1-aminoindan (●), (1R,2S)-(+)-*cis*-1-amino-2-indanol (□), (1S,2R)-(+)-*cis*-1-amino-2-indanol (■), (S)-(+)-indanol (◊) y (R)-(-)-indanol (○). (For experimental conditions, see the text).

Table 1 shows that the catalytic systems using (S)-(+)-1-aminoindan and (R)-(-)-1-aminoindan gave an excess of 63% and 45% of the enantiomer (R) of the reaction product. The *ee%* reached with the (S)-(+)-1-aminoindan modifier is comparable to that obtained in our laboratory using cinchonidine as modifier, under the same experimental conditions [40]. When (1S,2R)-(-)-*cis*-1-amino-2-indanol was used, *ee%* reached 30%, while for the reaction with (1R,2S)-(+)-*cis*-1-amino-2-indanol as modifier, *ee%* did not exceed 5%, with mainly (R)-ethyl lactate being obtained in both cases. The significant decrease of *ee%* in the reactions when these two modifiers are used may be due to the presence of an intramolecular hydrogen bond between one hydrogen atom of the

protonated amino group and the oxygen atom of the alcohol group in the molecules of both modifiers. Furthermore, when (S)-(+)-1-indanol and (R)-(-)-1-indanol were used as modifiers, very low *ee%* values were obtained, namely, <5% and 8%, respectively. These poor *ee%* values may be due to the absence of a basic nitrogen atom in the chiral modifier. As mentioned in the literature, in order for a molecule to act as chiral modifier, the presence of a basic nitrogen that can get protonated is an essential requirement. In other cases, it has been demonstrated that the absence of basic nitrogen substantially decreases *ee%*, and may even make it disappear. This behavior was noted by Blaser *et al.* when, on alkylating the quinuclidine nitrogen of the cinchonidine molecule, they found that the enantiodifferentiation was completely lost [45].

A remarkable observation that can be done about the *ee%* data shown in Table 1 is the existence of the so-called "inversion of enantioselectivity". That is, whatever the isomer of the chiral modifier used, mainly the same ethyl lactate enantiomer was obtained. This inversion of the sense of the enantioselectivity as compared to the expected sense based on the configuration of stereogenic center of the modifier has already been observed by several authors and is usually assigned to the stereochemistry of the adsorbed intermediate complex [46].

Theoretical calculations

In order to explain the experimental results, a series of computer calculations were performed. First, it was considered that the proton has a key role in the modifier–substract interactions as it is involved in the hydrogen bond formed between the modifier and the reactant. The proton affinity (PA) was calculated in order to get information on how feasible the protonation of each modifier is. The proton affinities calculated using equation (1) for the different modifiers are listed in **Table2**.

Table 2: Proton affinity (PA) calculated for the different modifiers at BLYP/TZP level of theory.

Modifier	***PA (kJ/mol)***
1-aminoindan	896.4
cis-1-amino-2-indanol	895.2
1-indanol	881.6

As expected, proton affinities calculated for each pair of isomeric modifiers yielded the same value within the calculation error. Thus, the PA value informed in Table 2 for "1-aminoindan" corresponds to the value obtained for both (S)-(+)-1-aminoindan and (R)-(-)-1-aminoindan modifiers. Likewise, PA values listed for "*cis*-1-amino-2-indanol" and "1-indanol" entries in Table 2 correspond to those calculated for each pair of isomers of both modifiers.

Calculations demonstrate that both 1-aminoindanes and *cis*-1-amino-2-indanols present a very similar proton affinity. Moreover, that value is higher than the proton affinity calculated for both 1-indanols. The difference is about 15 kJ/mol. These findings indicate that the amino groups present in both aminoindanol and aminoindan are the preferred sites for protonation when compared with the OH group in indanol, in agreement with previous reports on aromatic amino-alcohols [47].

According to current understanding, a one-to-one reactant–modifier complex is the source of enantiodifferentiation in the Orito reaction. The important reactant–modifier interaction takes place via a hydrogen bond between the carbonyl oxygen and proton bonded to quinuclidine nitrogen of the cinchonidine ($C{=}O\cdots HN^{+}$) [25,45,48,49]. This kind of hydrogen bond between an α-ketoester and a chiral modifier was observed experimentally by attenuated total reflection IR concentration modulation spectroscopy [50]. The source of enantiodifferentiation is the interaction between the protonated chiral modifier and the substrate. In this sense, in the theoretical calculations for this type of reaction, the protonated modifier has been commonly utilized as a starting point [24].

Taking into account that the protonated modifier is mandatory for the complex formation, this difference can explain the lowest *ee%* obtained using both indanol molecules as chiral modifiers **(Table1).** Hereafter, due to its low enantioselective activity, both indanols will not be taken into account in the modifier–substrate interaction calculations.

The interaction between ethyl pyruvate and (S)-(+)-1-aminoindan and between ethyl pyruvate and (1S,2R)-(-)-*cis*-1-amino-2-indanol was examined by means of computational modeling. The selected chiral modifiers correspond in each case, to the isomer with which the higher enantiomeric excess in the hydrogenation reaction of ethyl pyruvate was obtained. As an example, **Figure 4** shows four optimized geometries for the possible complexes formed between (S)-(+)-1-aminoindan and ethyl pyruvate. The optimized geometries for all the complexes formed by the two calculated modifiers and ethyl pyruvate are available as supplementary material. As aforementioned, although no DFT calculations on the metallic surface were performed, it is considered that both the chiral modifier and the substrate adsorb almost parallel to the surface. This is based on the assumption that the behavior of such modifiers is similar to that of cinchonidine molecules, a classical chiral modifier for this type of catalytic system. Experimental evidence from Near Edge X-Ray Absorption Fine Structure (NEXAFS) studies under ultrahigh vacuum (UHV) conditions indicates that cinchonidine molecules preferentially adsorb parallel to a Pt (111) surface [51].

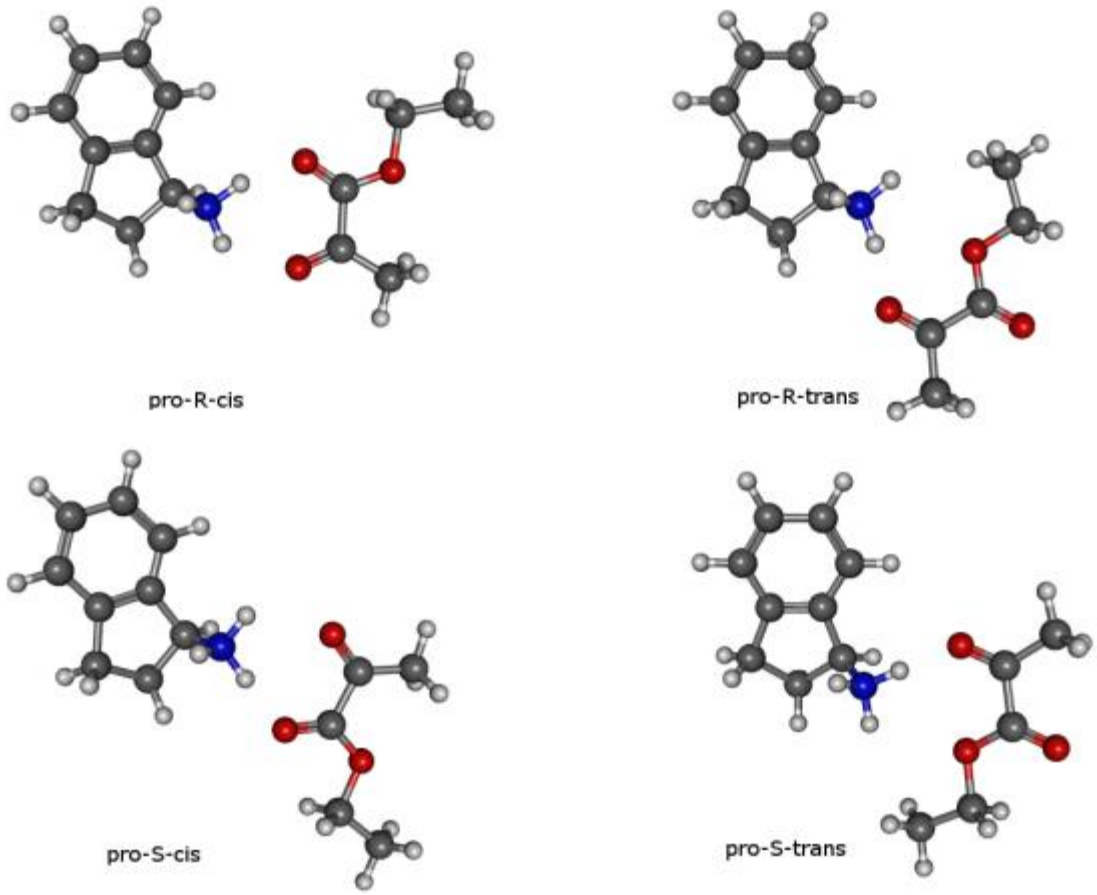

Figure 4. Optimized geometries for the complex formed between (S)-(+)-1-aminoindan and ethyl pyruvate.

The binding energies for each complex studied and the theoretically calculated *ee%* values, as well as the experimental *ee%* values, are listed in **Table 3**.

Table 3: ΔG_f (kJ·mol^{-1}) for each modifier-substrate complex studied, theoretical *ee %* calculated from a Maxwell-Boltzmann distribution (298 K) and experimental *ee %*.

Modifier	***Complex conformation***	***ΔG_f (kJ·mol^{-1})***	***ee%[a] (calc)***	***ee% (exp)***
(S)-(+)-1-aminoindan	pro-R-*cis*	173.93	81.37 (R)	63 (R)
	pro-R-*trans*	194.89		
	pro-S-*cis*	179.58		
	pro-S-*trans*	200.87		
(1S,2R)-(-)-cis-1-amino-*2*-indanol	pro-R-*cis*	54.77	24.37 (R)	30 (R)
	pro-R-*trans*	65.60		
	pro-S-*cis*	56.15		
	pro-S-*trans*	62.51		

[a]Calculated using equation (4).

Regardless of the modifier used, the complexes where the substrate is in *cis* conformation always have a lower ΔG_f than in *trans* conformation. This may be because when the substrate has a *cis* conformation, it can interact through two carbonyl oxygen atoms with the hydrogen atom of the protonated amino group. In the case of complexes formed by *trans* isomers, the longer distance between the oxygen atom of the substrate ester group and the amino group hydrogen atom of the modifier would generate very weak interactions compared to those of the complexes involving the substrate en the *cis* conformation.

The calculated *ee%* values are very close to the experimental ones, and in all cases an excess of the *R* enantiomer was predicted, as was observed in the experimental tests. Moreover, all the calculated binding energies for complex formation between the (S)-(+)-1-aminoindan are greater than the ΔG_f calculated for the complexes formed between the substrate and (1S,2R)-(-)-*cis*-1-amino-2-indanol.

In order to explain the decrease in *ee%* when both aminoindanols were used as modifiers, the possible intramolecular hydrogen bridge bonding, hindering complex formation between the substrate and these two modifiers, was examined. **Figure 5** shows the binding lengths and angles between the oxygen atom of the hydroxyl group and its closest hydrogen atom of the protonated amino group.

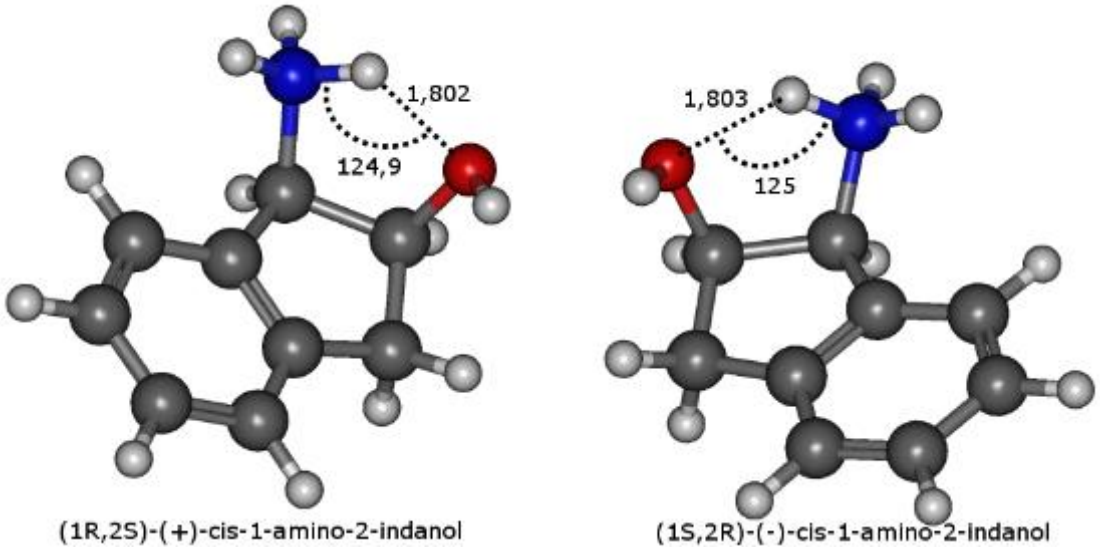

Figure 5. Binding lengths between the oxygen atom of the hydroxyl group and its closest hydrogen atom of the protonated amino group (Å) and bond angle between N-H-O for both aminoindanol molecules.

From the values of these calculated parameters, it follows that in both aminoindanol molecules there exist moderate to weak hydrogen bridge bonds based on Jeffrey's classification [52]. The bond length obtained falls within the range of –N-H···O bond lengths described as characteristic of moderate strength bonds by Szatyłowicz [53].

Figure 6 shows the most stable structures for the (1R,2S)-(+)-*cis*-1-amino-2-indanol and (1S,2R)-(-)-*cis*-1-amino-2-indanol molecules calculated from the graph of the 3D analysis of noncovalent interactions. In agreement with Zehnacker *et al.* [54], a

bicolored isosurface, typical of intramolecular hydrogen bonding, is observed. The red isosurface, which corresponds to a negative λ_2 value, between the oxygen atom and the hydrogen atom of the protonated amino group, clearly indicates the presence of intramolecular hydrogen bonding. The blue zones, with a positive λ_2 value, at the center of both rings, correspond to repulsive interactions characteristic of the steric repulsions deriving from ring formation. The green isosurface represents a zone where the reduced gradient is close to zero. A zone between a hydrogen atom of the protonated amino group and another hydrogen atom bonded to an aromatic ring carbon is observed in both molecules. The zones where the reduced gradient is close to zero are characteristic of weak van der Waals interactions.

The NCI analysis revealed intramolecular hydrogen bonding. Due to this intramolecular bonding, the protons of the protonated amino group, which are essential for complex formation between the chiral modifier and the substrate, become less available. This would lead to a decrease in *ee%* when these chiral modifiers are used. However, the R enantiomer is preferentially formed in both cases.

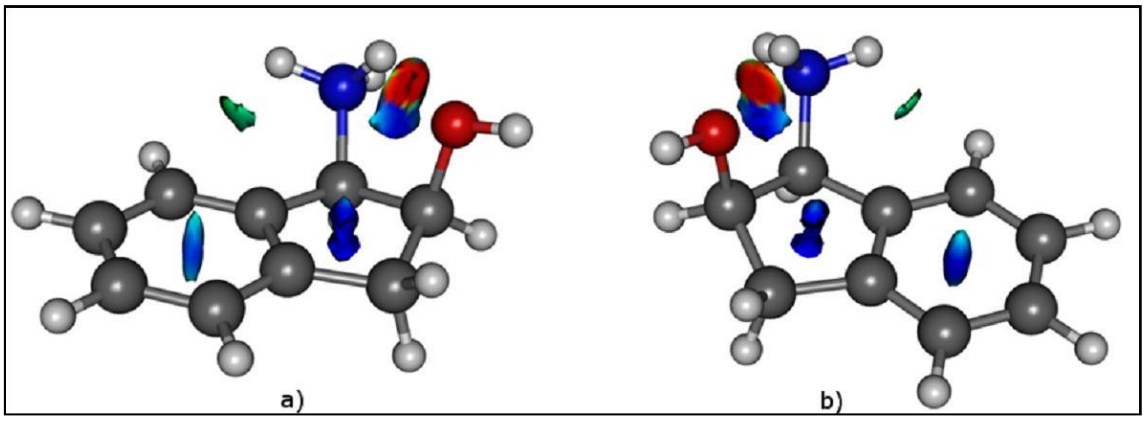

Figure 6. The most stable structures for (1R,2S)-(+)-*cis*-1-amino-2-indanol (a) and (1S,2R)-(-)-*cis*-1-amino-2-indanol (b), with their respective isosurfaces calculated through NCI analysis. (For interpretation of the colors in this figure, the reader is referred to the web version of this article).

CONCLUSIONS

Six new non-cinchona chiral modifiers for the enantioselective hydrogenation reaction of ethyl pyruvate were studied. They are smaller, more rigid and simpler than cinchonidine, the most efficient and widely used chiral modifier for this reaction. With the four modifiers that have a basic nitrogen atom in their structure, an enantiomeric excess (*ee%*) of the (R)-ethyl lactate isomer was obtained. When the chiral modifier used did not have a basic nitrogen atom in its structure, as in (S)-(+)-1-indanol and (R)-(-)-1-indanol, which is essential for the enantiodifferentiation, the *ee%* values were very low.

Theoretical calculations indicated that the alcohol group in indanols has a smaller proton affinity than the amino groups of aminoindans and aminoindanols. This is the reason why basic nitrogen that can be protonated is required for complex formation with the substrate to be hydrogenated.

With a simple model, where the metallic surface was not explicitly considered, and a low computational cost, theoretical results may accurately predict the experimental *ee%* values. From theoretical calculations and an NCI analysis, intramolecular hydrogen bonding was also proven. This intramolecular hydrogen bond is responsible for the decrease in *ee%* compared to the results arrived at when the aminoindans were used as chiral modifiers.

ACKNOWLEDGEMENTS

The authors thank the Consejo Nacional de Investigaciones Científicas y Técnicas (CONICET) for grant PIP 0276 and the Universidad Nacional de La Plata (Projec X700) for institutional support.

REFERENCES

[1] S.C. Stinson, Chem. Eng. News 79 (2001) 79.

[2] A.M. Rouhi, Chem. Eng. News 81 (2003) 45.

[3] A.M. Rouhi, Chem. Eng. News 82 (2004) 47.

[4] H.U. Blaser, F. Spindler, M. Studer, Appl. Catal. A 221 (2001) 119-143.

[5] H.U. Blaser, M. Studer, Chirality 11 (1999) 459-464.

[6] T. Osawa, T. Harada, O. Takayasu, Top. Catal. 13 (2000) 155-168.

[7] Y. Izumi, Adv. Catal. 32 (1983) 215-271.

[8] D.Y. Murzin, P. Maki-Arvela, E. Toukoniitty, T. Salmi, Catal. Rev. Sci. Eng. 47 (2005) 175-256.

[9] H.U. Blaser, H.-P. Jalett, F. Spindler, J. Mol. Catal. A: Chem. 107 (1996) 85-94.

[10] Y. Orito, S. Imai, S. Niwa, G.H. Nguyen, Synth. Org. Chem. Jpn. 37 (1979) 173-174.

[11] G. Szőllősi, K. Balázsik, I. Bucsi, T. Bartók, M. Bartók, Catal. Comm. 32 (2013) 81-85.

[12] C. Mondelli, C. Bucher, A. Baiker, R. Gilmour, J. Mol. Catal. A: Chem. 327 (2010) 87-91.

[13] G. Szőllősi, S. Cserényi, I. Bucsi, T. Bartók, F. Fülöp, M. Bartók, App. Catal. A: Gen. 382 (2010) 263-271.

[14] H. Pan, X. Li, D. Zhang, Y. Guan, P. Wu, J. Mol. Catal. A: Chem. 377 (2013) 108-114.

[15] C.H. Campos, C. Torres, J.L. García Fierro, P. Reyes, App. Catal. A 466 (2013) 198-207.

[16] M.U. Azmat, Guo, Y. Guo, Y. Guo, Y. Wang, G. Lu, *J. Mol. Catal. A: Chem.* 336 (2011) 42-50.

[17] K. Balázsik, M. Bartók, J. Catal. 224 (2004) 463-472.

[18] R.J. LeBlanc, W. Chu, C.T. Williams, J. Mol. Catal. A: Chem. 212 (2004) 277-289.

[19] D. Ferri, T. Bürgi, J. Am. Chem. Soc. 123 (2001) 12074-12084.

[20] A.F. Carley, M.K. Rajumon, M.W. Roberts, P.B. Wells, J. Chem. Soc., Faraday Trans. 91 (1995) 2167-2172.

[21] J.M. Bonello, E.C.H. Sykes, R. Lindsay, F.J. Williams, A.K. Santra, R.M. Lambert, Surf. Sci. 482–485 (2001) 207.

[22] T. Bürgi, F. Atamny, R. Schlögl, A. Baiker, J. Phys. Chem. B 104 (2000) 5953-5960.

[23] T. Bürgi, F. Atamny, A. Knop-Gericke, M. Hävecker, T. Schedel-Niedrig, R. Schlögl, A. Baiker, Catal. Lett. 66 (2000) 109-112.

[24] T. Bürgi, A. Baiker, J. Catal. 194 (2000) 445-451.

[25] A. Baiker, J. Mol. Catal. A: Chem. 163 (2000) 205-220.

[26] J. Walkimar de M. Carneiroa, C. da S.B. de Oliveira, F. B. Passos,D. A.G. Aranda, P. R. N. de Souza, O.A.C. Antunes, J. Mol. Catal. A: Chem 226 (2005) 221-226.

[27] E. Tálas, J.L. Margitfalvi, Chirality 22 (2010) 3–15 and references cited therein.

[28] P. Kukula, V. Matoušek, T. Mallat, A. Baiker, Tetrahedron: Asymmetry 18 (2007) 2859–2868.

[29] A. B. Merlo, J. F. Ruggera, G. F. Santori, A. Moglioni, G. Y. Moltrasio Iglesias, M. L. Casella, O. A. Ferretti, Catal. Tod. 133–135 (2008) 654-660.

[30] A.D. Beke, J. Chem. Phys. 98 (1993) 1372-1377.

[31] C. Lee, W. Yang, R.G. Parr, Phys Rev. A, 37 (1988) 785-789.

[32] (a) ADF2004.01, SCM, Theoretical Chemistry, Vrije Universiteit, Amsterdam, The Netherlands. Available from: <http://www.scm.com>.

(b) C. Fonseca Guerra, J.G. Snijders, G. te Velde, E.J. Baerends, Theor. Chem. Acc. 99 (1998) 391-403.

(c) G. te Velde, F.M. Bickelhaupt, S.J.A. van Gisbergen, C. Fonseca Guerra, E.J. Baerends, J.G. Snijders, T. Ziegler, J. Comput. Chem. 22 (2001) 931-967.

[33] C.C. Pye, T. Ziegler, E. van Lenthe, J.N. Louwen, *An implementation of the conductor-like screening model of solvation within the Amsterdam density functional package. Part II. COSMO for real solvents*, Can. J. Chem. 87 (2009) 790-797.

[34] E. R. Johnson, S. Keinan, P. Mori-Sanchez, J. Contreras-Garcia, A. J. Cohen and W. Yang, J. Am. Chem. Soc. 132 (2010) 6498-6505.

[35] J. Contreras-Garcia, W. T. Yang and E. R. Johnson, J. Phys.Chem. A 115 (2011) 12983-12990.

[36] R. Chaudret, B. d. Courcy, J. Contreras-Garcia, E. Gloaguen, A. Zehnacker-Rentien, M. Mons and J. P. Piquemal, Phys. Chem. Chem. Phys. 16 (2014) 9876-9891.

[37] A.R. ALLOUCHE, Gabedit is a free Graphical User Interface for computational chemistry packages. It is available from http://gabedit.sourceforge.net/

[38] J.T. Wehrli, A. Baiker, D.M. Monti, H.U. Blazer, J. Mol. Catal. 61 (1990) 207-226.

[39] E. Toukoniitty, P. Mäki-Arvela, A. Kalantar Neyestanaki, T. Salmi, A. Villela, R. Leino, R. Sjöholm, E. Laine, J. Väyrynen, T. Ollonqvist, Stud. Surf. Sci. Catal. 130 (2000) 3363-3368.

[40] L. W. Ho, C. P. Hwang, J. F. Lee, I. Wang, C. T. Yeh, J. Mol. Catal. A: Chem. 136 (1998) 293-298.

[41] J. T. Wehrli, A. Baiker, D. M. Monti, H.U. Blaser, H. P. Jalett, J. Mol. Catal. 57 (1989) 245-257.

[42] U. Blaser, H. P. Jalett, J. Wiehl, J. Mol. Catal. A: Chem. 68 (1991) 215-222.

[43] S. Cserényi, I. Bucsi, K. Felföldi, K. Balázsik, G. Szöllösi, M. Bartók, J. Mol. Catal. A: Chem. 247 (2006) 108-115.

[44] S. Cserényi, I. Bucsi, K. Felföldi, React. Kinet. Catal. Lett. 87 (2005) 395-403.

[45] K. Szőri, K. Balázsik, S. Cserényi, G. Szőllősi, M. Bartók, Applied Catalysis A: General 362 (2009) 178–184

[46] H.U. Blaser, H.P. Jalett, W. Lottenbach, M. Studer; J. Am. Chem. Soc., 122 (2000) 12675-12682.

[47] G. Bouchoux and J. Y. Salpin, Mass Spectrom. Rev. 31 (2012) 353-390.

[48] M. vonArx, T. Mallat, A. Baiker, Top.Catal. 19 (2002) 75-87.

[49] M. Studer, H.-U. Blaser, C. Exner, Adv. Synth. Catal. 345 (2003) 45-65.

[50] N. Bonalumi, T. Burgi, A. Baiker, J. Am. Chem. Soc. 125 (2003) 13342-13343.

[51] T. Evans, A.P. Woodhead, A. Gutiérrez-Sosa, G. Thornton, T.J. Hall, A.A. Davis, N.A. Young, P.B. Wells, R.J. Oldman, O. Plashkevych, O. Vahtras, H. Ågren, V. Carravetta, Surf. Sci., 436 (1999) L691-L696.

[52] G.A. Jeffrey, An introduction to hydrogen bondig, Oxford University Press: Oxford, 1997.

[53] H. Szatyłowicz, J. Phys. Org. Chem. 21 (2008) 897-914.

[54] A. Bouchet, J. Klyne, G. Piani, O. Dopfer, A. Zehnacker, Phys. Chem. Chem. Phys. 17 (2015) 25809-25821.

Figure Captions

Scheme 1. Chemical structures of the chiral modifiers studied

Figure 1. Enantioselective hydrogenation of ethyl pyruvate to (R) and (S)-ethyl lactate

Figure 2. TEM image of Pt/SiO_2 catalyst

Figure 3. Hydrogenation reaction of ethyl pyruvate in 2-propanol. Conversion as a function of time for the Pt/SiO_2 catalyst without modifier (×) and modified with: (S)-(+)-1-aminoindan (▲), (R)-(-)-1-aminoindan (●), (1R,2S)-(+)-*cis*-1-amino-2-indanol (□), (1S,2R)-(+)-*cis*-1-amino-2-indanol (■), (S)-(+)-indanol (◊) y (R)-(-)-indanol (○). (For experimental conditions, see the text).

Figure 4. Optimized geometries for the complex formed between (S)-(+)-1-aminoindan and ethyl pyruvate.

Figure 5. Binding lengths between the oxygen atom of the hydroxyl group and its closest hydrogen atom of the protonated amino group (Å) and bond angle between N-H-O for both aminoindanol molecules.

Figure 6. The most stable structures for (1R,2S)-(+)-*cis*-1-amino-2-indanol (a) and (1S,2R)-(-)-*cis*-1-amino-2-indanol (b), with their respective isosurfaces calculated through NCI analysis. (For interpretation of the colors in this figure, the reader is referred to the web version of this article).